GENERATIVE COMPRESSION FOR FACE VIDEO: A HYBRID SCHEME

Anni Tang, Yan Huang*, Jun Ling*, Zhiyu Zhang*, Yiwei Zhang*, Rong Xie*, Li Song*,† ✉*

*Institute of Image Communication and Network Engineering, Shanghai Jiao Tong University, China
†MOE Key Lab of Artificial Intelligence, AI Institute, Shanghai Jiao Tong University, China
{memory97, 2250344200, lingjun, zhiyu-zhang, 6000myiwei, xierong, song_li}@sjtu.edu.cn

arXiv:2204.10055v3 [eess.IV] 20 Mar 2023

ABSTRACT

As the latest video coding standard, versatile video coding (VVC) has shown its ability in retaining pixel quality. To excavate more compression potential for video conference scenarios under ultra-low bitrate, this paper proposes a bitrate-adjustable hybrid compression scheme for face video. This hybrid scheme combines the pixel-level precise recovery capability of traditional coding with the generation capability of deep learning based on abridged information, where Pixel-wise Bi-Prediction, Low-Bitrate-FOM and Lossless Keypoint Encoder collaborate to achieve PSNR up to 36.23 dB at a low bitrate of 1.47 KB/s. Without introducing any additional bitrate, our method has a clear advantage over VVC under a completely fair comparative experiment, which proves the effectiveness of our proposed scheme. Moreover, our scheme can adapt to any existing encoder/configuration to deal with different encoding requirements, and the bitrate can be dynamically adjusted according to the network condition.

***Index Terms*—** face video, video compression, versatile video coding, deep generation, generative compression

1. INTRODUCTION

In the context of COVID-19, more and more video calls are made, and face video compression technologies are becoming increasingly significant. In the case of poor network quality, achieving stable and smooth video call with ultra-low bitrate is a hot research topic. Existing methods for face video compression can be divided into two categories: traditional coding methods and deep-learning-based methods.

Traditional video coding methods have the advantage of pixel-level precise recovery even for rapidly changing scenes, where VVC [1] is the most advanced standard. Compared with HEVC [2], VVC saves about 50% of the bitrate while maintaining the similar visual quality. However, these traditional methods represented by VVC do not discriminate video content and compress all videos in the same way although in fact, face video compression should have more potential.

Deep learning has the generation capability based on abridged information, so it has great potential in face video compression. Researchers have proposed some deep-learning-based methods [3–5] to implement face video compression. Oquab et al. [5] designed a mobile-compatible architecture based on FOM [6], but bad results may appear with large attitude changes due to fixed reference frames. Wang et al. [4] proposed an one-shot neural talking-head synthesis approach which utilizes one reference frame to generate a free-view output video, but the objective quality is not that satisfactory. Feng et al. [3] proposed a video compression framework that utilizes pre-saved face frames as reference to reconstruct the target frame with fine details, where additional bitrates are introduced which leads to unfair bitrate comparison. The above methods [3–5, 7] apply static reference frames, so it's hard to guarantee good performance in case of scene switch or large attitude transformation, which leads to a failure in high fidelity recovery. There also exists a generative compression method [7] based on FOM [6], utilizing one raw frame as reference and adding the generated frames to the reference frame pool, which tends to cause error accumulation. However, pixel-level accurate recovery is the strength of traditional coding methods. Consequently, we come up with the idea of designing a hybrid scheme which combines traditional coding with deep generation. Moreover, most of the existing AI-based video conference methods can hardly dynamically adjust the bitrate. For example, these methods [3–5, 7] can only adjust the bitrate through adjusting the number of keypoints despite the fact that different numbers of keypoints correspond to different models, further limiting their practicality.

To tackle the aforementioned problems, we propose a bitrate-adjustable hybrid coding scheme. It is a hybrid scheme because we sample the key frames according to a certain frequency, encode these key frames with traditional method such as VVC, and use deep generative method to reconstruct non-key frames according to the transmitted keypoints. Combining the pixel-level recovery capability of traditional coding with the detail generation capability of deep learning, our proposed hybrid scheme is able to synthesize high-quality face videos at ultra-low bitrate. Meanwhile, the bitrate can be dynamically adjusted through two channels: the sampling interval of key frames or the compression ratio of key frames. Thus, we can dynamically choose the right configuration according to the network condition, which is more practical than

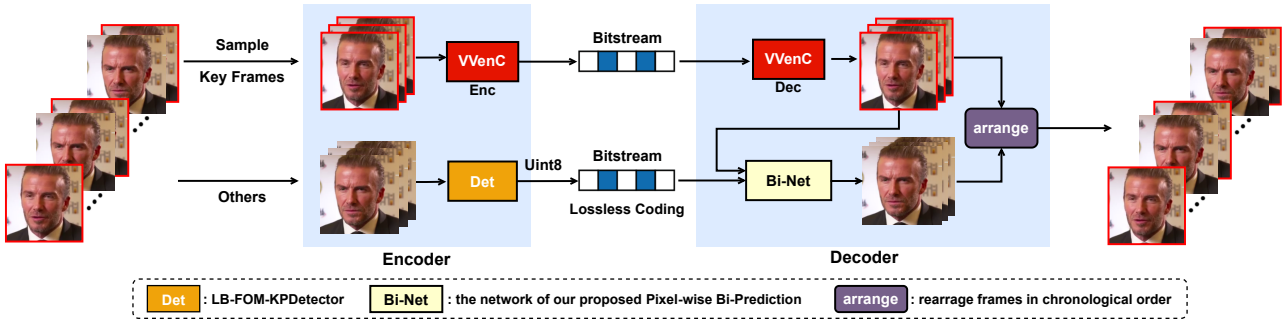
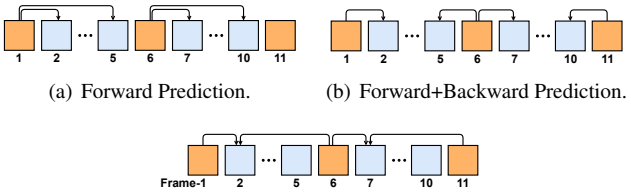


Fig. 1: Overview of our method. *Sender*: (1) Sample key frames according to a certain sampling interval and use VVenC to encode them. (2) Extract keypoints of each non-key frame and encode them losslessly. (3) Transmit the VVenC and keypoint bitstream. *Receiver*: (1) Decode the VVenC bitstream to get key frames. (2) Use the decoded key frames and the decoded keypoints of non-key frames to reconstruct the non-key frames via Bi-Net. (3) Rearrange all frames in chronological order.



(a) Forward Prediction. (b) Forward+Backward Prediction.

(c) Pixel-wise Bi-Prediction.

Fig. 2: Three prediction methods. Assuming the sampling interval is 5, the orange blocks are key frames and the blue ones are non-key frames. In (a), a non-key frame is predicted by the previous key frame. In (b), a non-key frame is predicted by the key frame closest to it. In (c), a non-key frame is predicted by two adjacent key frames jointly.

the aforementioned methods.

In our scheme, inspired by bidirectional prediction idea of traditional coding, we design a Pixel-wise Bi-Prediction method shown in Figure 2(c), which uses two adjacent key frames and the keypoints of non-key frames to predict the non-key frames, greatly improving the smoothness of the generated video. Specifically, we selected FOM [6] as the basic generation model since it utilizes a sparse representation of human faces to implement face animation which costs a relatively-low bandwidth compared to [8–11]. Based on FOM [6], we propose a low bitrate version called LowBitrate-FOM (LB-FOM) to further lower the bitrate, taking the bitrate to one-twelfth of original FOM [6] with little loss of quality, and design a lossless coding scheme to conduct further compression. Overall, we assist traditional coding with deep generative methods to improve the detail retention and assist deep generative methods with traditional bidirectional prediction idea to improve smoothness, achieving the goal of generating smooth and detailed face video at ultra-low bitrate.

Our method does not introduce any additional bitrate, which means there is not any prior information at the receiver such as pre-saved reference frames before transmission. Thus, under a completely fair comparison, our method has an obvious advantage over VVC in face video compression, which proves the effectiveness of our proposed scheme. Moreover, our scheme applies to any existing encoder/configuration, to deal with different encoding requirements. The contributions can be summarized as: (1) We propose a hybrid compression scheme for face video which combines the advantages of traditional coding and deep learning, synthesizing high quality face video at ultra-low bitrate. (2) A Pixel-wise Bi-Prediction method is proposed to generate smooth videos. (3) We propose an LB-FOM which takes the bitrate to one-twelfth of original FOM [6] with little loss of quality. (4) Our scheme implements dynamically-adjustable bitrate and adapts to any existing encoder/configuration to deal with different encoding requirements.

2. METHOD

For a video sequence, at the sender, we sample the key frames according to a certain frequency (e.g., take one key frame every 5 frames), encode these key frames with VVenC [12], an efficient VVC realization which has compression performance similar to VVC but with much less encoding complexity, and transmit the bitstream to the receiver. For non-key frames, we use the proposed LB-FOM-KPDetector in Figure 4(b) to detect keypoints of type Uint8, encode them losslessly and transmit the bitstream to the receiver. At the receiver, the bitstream of VVenC is decoded to reconstruct the key frames. With the reconstructed key frames and the keypoints of the non-key frames, we utilize Bi-Net, the network of the proposed Pixel-wise Bi-Prediction method, to reconstruct the non-key frames. The network architecture is illustrated in Section 2.1. Finally, we rearrange all frames in chronological order to get the final video streaming at the receiving end. Details of the lossless coding scheme and bitrate calculation will be explained in Section B.

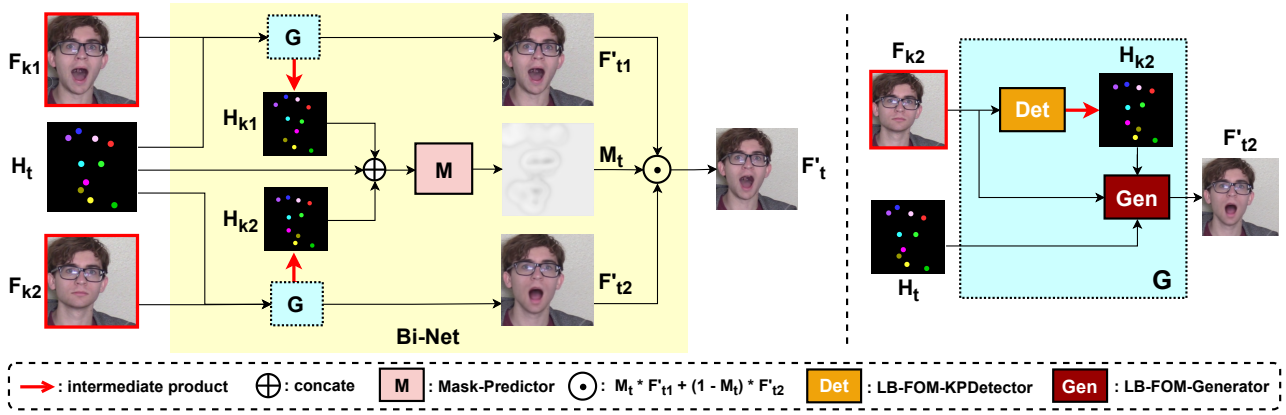
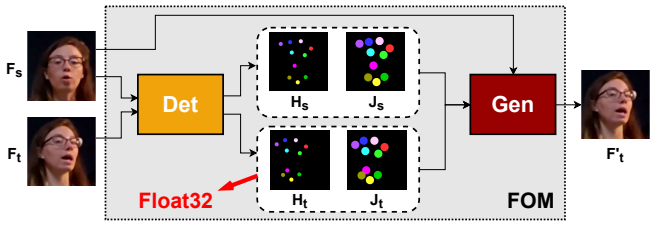
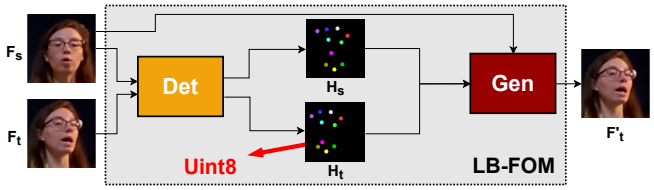


Fig. 3: Architecture of the proposed Bi-Net. According to two adjacent key frames (F_{k1} and F_{k2}) and the keypoint heatmap (H_t) of the intermediate non-key frame (F_t), we can reconstruct F_t via Bi-Net.



(a) Architecture of FOM [6].



(b) Architecture of LB-FOM.

Fig. 4: The architecture of FOM [6] and LB-FOM.

2.1. Bi-Net: Pixel-wise Bi-Prediction

In Figure 2, Forward Prediction tends to lead to obvious jitter between the 5th and 6th frame, and Forward+Backward Prediction tends to lead to obvious jitter between the 3rd and 4th frame, damaging our subjective experience, which has been proved in Table 4. Thus, we propose a Pixel-wise Bi-Prediction method and design a Bi-Net to implement this idea.

As shown in Figure 3, overall, the input of Bi-Net is two adjacent key frames (F_{k1} and F_{k2}) and the keypoint heatmap of a non-key frame (H_t), and the output is the predicted non-key frame F'_t corresponding to H_t. Specifically, we feed F_{k1} and H_t to G to get the intermediate product H_{k1} and the reenacted result F'_{t1}. In the same way, F_{k2} and H_t are fed to G to get H_{k2} and F'_{t2}. Then, the concatenation of H_{k1}, H_t and H_{k2} is fed to the Mask-Predictor with an encoder-decoder architecture to predict a mask M_t with value between 0 and 1 which acts on F'_{t1} and F'_{t2}, obtaining the final result F'_t:

$$F'_t = M_t * F'_{t1} + (1 - M_t) * F'_{t2}. \quad (1)$$

Table 1: The comparison of FOM [6] and LB-FOM in bitrate and image synthesis quality.

Method	Jac	dType	noise	Bytes/frame ↓	PSNR(Y) ↑
FOM [6]	Yes	Float32	-	240	**36.76**
FOM w/o Jac	No	Float32	-	80	36.28
LB-FOM w/o noise	No	Uint8	No	**20**	36.06
LB-FOM	No	Uint8	Yes	**20**	36.47

The architecture of G is shown at the right of Figure 3, and the details of LB-FOM is illustrated below.

LB-FOM Siarohin et al. proposed FOM [6] to implement face animation. As shown in Figure 4(a), FOM [6] utilizes a KPDetector to predict the keypoints H_s and corresponding Jacobian J_s of the source image F_s, and predict the keypoints H_t and corresponding Jacobian J_t of the target image F_t, where all data is of type Float32. Then H_s, J_s, H_t, J_t and the source image F_s are fed to the generator to obtain the final result F'_t.

In FOM [6], each frame is represented by a fixed number of keypoints (e.g. 10) along with their Jacobians. Each keypoint consists of an (x, y) coordinate, and the corresponding Jacobian is of size 2×2. Since all data is of type Float32, for each frame, the keypoints are represented by 80 Bytes and the Jacobians are represented by 160 Bytes, resulting in a total bitrate of 240 Bytes/frame.

To lower the bitrate, we propose a LowBitrate-FOM (LB-FOM) in Figure 4(b). Specifically, we remove the prediction of Jacobians and quantify the keypoints in [-1,1] into range [0, 255], which means data of type Float32 is converted to type Uint8. In this way, the total bitrate decreases from 240 Bytes/frame to 20 Bytes/frame. Table 1 shows the impact of such cuts. In Table 1, removing the Jacobian and converting Float32 to Uint8 directly lead to the continuous decline of PSNR, from 36.76 dB to 36.28 dB to 36.06 dB. This is probably because direct quantization is non-differentiable, resulting in the failure of gradient back propagation. When



Fig. 5: The reconstructed images using VVenC and our method under the same bitrate. Mode: *RA*, sampling-interval:10

we add uniform noise to the predicted keypoints to simulate the quantization loss in the training phase, the PSNR value decreases only 0.29 dB compared to the original FOM [6], while the bitrate is reduced to one-twelfth of it, which is a good deal, demonstrating the effectiveness of our proposed LB-FOM. An ablation study is conducted in Table 5 to further explore the issue about keypoints quantization.

2.2. Training Schemes

First, we take two frames from the same video at a time as paired training data and train LB-FOM in a supervised manner with (5). After training LB-FOM, fix the weights of it, that is, fix G, and train the Mask-Predictor to predict a valid mask M_t which acts on F'_{t1} and F'_{t2} to synthesize the final F'_t with (5). Specifically, we take three frames from the same video at a time, and let the intermediate frame as the non-key frame and the rest two frames as the key frames. After training the Mask-Predictor, finetune the whole Bi-Net for a few epochs. Finally, quantify the keypoints directly rather than use uniform noise to simulate the quantization loss, and finetune another epoch to further improve the performance.

Loss functions. We use L1, L2 and perceptual loss [13] to optimize our model:

$$L_1 = \|F'_t - F_t\|_1, \tag{2}$$

$$L_2 = \|F'_t - F_t\|_2, \tag{3}$$

$$L_{perc} = \sum_{i=1}^{n} \left\|\mathrm{VGG}_i\left(F_t\right) - \mathrm{VGG}_i(F'_t)\right\|_1, \tag{4}$$

where i is the selected layer indexes of VGG19. Full loss:

$$L_{full} = \lambda_1 \cdot L_1 + \lambda_2 \cdot L_2 + \lambda_{perc} \cdot L_{perc}, \tag{5}$$

where λ_1=λ_2=λ_{perc}=10.

2.3. Lossless Coding Scheme and Bitrate Calculation

In this paper, LB-FOM predicts 10 keypoints of type Uint8 for each non-key frame, so each non-key frame is represented by 20 Bytes if uncompressed. To encode these keypoints, we design a lossless coding scheme, in which way each non-key frame is compressed to 4.98 Bytes on average. Specifically, we utilize intra and inter prediction, exponential Golomb coding and adaptive binary arithmetic coding [14] to further reduce the bitrate. More details can be found in $Sup.Mat.$.

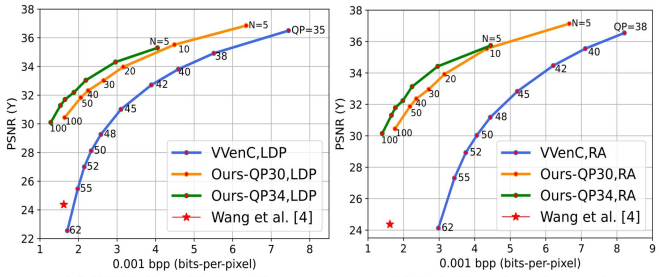
The total bitstream is composed of two parts: VVenC bitstream from key frames and keypoint bitstream from non-key frames. The sampled key frames are treated as a new video and VVenC is utilized to encode this video. The bitstream is determined by VVenC algorithm [12]. As mentioned above, each non-key frame is represented by 4.98 Bytes on average with our lossless coding scheme. Assuming that the sampling interval is N, which means there is one key frame in every N frames, we can calculate the average bitrate:

$$B_{avg} = [B_k * 1 + B_{nk} * (N-1)]/N, \tag{6}$$

where B_k is the bitrate of the key frame, B_{nk} is the bitrate of the non-key frame, and B_{avg} is the average bitrate.

Table 2: The quantitative results corresponding to Figure 5. bpp: bits-per-pixel, KB/s: 1024-Bytes-per-second. "Ours-QP34-N10" means the sampling interval is 10 and for key frames encoded by VVenC, the QP value is 34. The corresponding compressed videos can be seen in $Sup.Mat.$.

Method	Bitrate		PSNR(Y)	User Study	
	10^{-3}bpp	KB/s		Fidelity	Aesthetics
VVenC-QP62	2.97	0.71	24.13	0.00	0.00
Ours-QP34-N10	2.96	0.71	**34.42**	**1.00**	**1.00**
VVenC-QP52	3.76	0.90	28.93	0.00	0.00
Ours-QP32-N10	3.55	0.85	**35.04**	**1.00**	**1.00**
VVenC-QP42	6.21	1.49	34.47	0.15	0.00
Ours-QP27-N10	6.12	1.47	**36.23**	**0.85**	**1.00**
VVenC-QP42	6.21	1.49	34.47	0.16	0.18
Ours-QP34-N10	**2.96**	**0.71**	34.42	**0.84**	**0.82**



(a) LDP (LowDelay-P) (b) RA (RandomAccess)

Fig. 6: The performance comparison of VVenC and our method in both *LDP* and *RA* mode. *LDP*: BD-rate = **-43.12%**, *RA*: BD-rate = **-58.48%**.

3. EXPERIMENTS

3.1. Implementation Details

Datasets. In this paper, we use DFDC [15] as our trainset. DFDC dataset consists of over 15,000 face videos and each video consists of nearly 300 frames. To test our method, we download 15 videos from YouTube in VoxCeleb2 [16] as our testset, and each video consists of nearly 300 frames. All experiments were conducted at 256×256 image resolution, while Table 3 further shows some experimental results at 512×512 resolution. For all videos, frame rate is 30 FPS.

Metrics. We use PSNR(Y) (in dB), the Peak Signal-to-Noise Ratio value of Y channel in yuv format, as the main objective metric. For subjective metrics, in Table 2, *fidelity* score reflects the degree of detail retention and *aesthetics* score reflects the overall video visual quality. Specifically, we simultaneously show two videos encoded by VVenC and our method respectively and tell the users to choose the better one in fidelity or aesthetics, so the score is actually the user preference percentage. In Table 4 and Table 5, the *smoothness* score reflects the degree of video smoothness and fluency. These methods are compared in pairs. For each method, *smoothness*-score = the number of times it was preferred / the total number of times it was compared.

Table 3: More results at 256×256 and 512×512 resolutions. Mode: *RA*. KB/s: 1024-Bytes-per-second. "Ours-QP34-N30" means the sampling interval is 30 and for key frames encoded by VVenC, the QP value is 34.

Method	256×256		512×512	
	KB/s	PSNR(Y)	KB/s	PSNR(Y)
VVenC-QP62	0.71	24.13	0.82	26.82
VVenC-QP52	0.90	28.93	1.23	31.92
Ours-QP34-N30	0.48	32.24	0.86	31.59
Ours-QP36-N30	0.42	31.87	0.74	31.49
Ours-QP36-N10	0.60	33.81	1.13	33.47

Table 4: An ablation study on three prediction methods.

Method	Forward	Forward+Backward	Pixel-wise Bi-Prediction
PSNR(Y)	35.45	36.05	**36.47**
Smoothness	0.021	0.083	**0.937**

3.2. Comparison Results

We mainly compare our proposed method with VVenC in Figure 5 and Figure 6. As shown in Figure 5, at the same bitrate, the visual quality of our generated images are obviously better than that of VVenC. For example, at the bitrate of 0.7 KB/s, VVenC obtained the performance of QP=62, while in our method, we encoded the key frames at QP=34 and generated the non-key frames almost with the same quality as the key frames, that is, cost the bitrate of QP=62 while achieved the quality of QP=34. Specific values of bitrate and PSNR are shown in Table 2, where the results demonstrate that our method achieves obviously better performance than VVenC in detail retention and overall quality. Additionally, we show more results at 256×256 and 512×512 resolutions in Table 3. Complete experimental data is shown in $Sup.Mat.$.

Figure 6 shows the quantitative results in *LDP* mode and *RA* mode. Without the loss of generality, we take Figure 6(a) as example. We choose VVenC as our baseline, and test its performance from QP=35 to QP=62. Higher QP value means higher compression ratio. As mentioned above, our method can implement dynamically-adjustable bitrate through two channels: adjust the sampling interval of key frames or adjust the compression ratio (that is, QP value) of key frames. In Figure 6(a), the orange broken line shows the performance of different sampling intervals from 5 to 100 under QP=30, and the green broken line is the performance under QP=34. In fact, QP value and the sampling interval can be determined freely, not limited to those listed. In addition, we also compared our method with Wang et al. [4]. Since there is no released test code, we applied the data released in their paper and drew it in Figure 6. It can be found that our method achieves significantly better performance than VVenC and Wang et al. [4] in either *LDP* mode or *RA* mode.

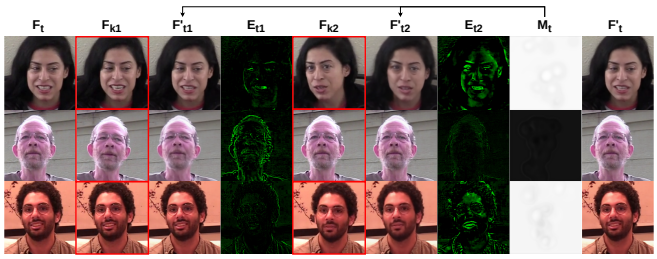


Fig. 7: The intermediate products generated in the inference process. F_t is the target non-key frame to be generated. F_{k1} & F_{k2} are two adjacent key frames, and F'_{t1} & F'_{t2} are their predictive results using G, respectively. E_{t1} is the error map between F_t and F'_{t1}, and E_{t2} is the error map between F_t and F'_{t2}. M_t is the predicted mask which operates on F'_{t1} and F'_{t2}. F'_t is the final synthesized result.

Table 5: An ablation study on the quantization of keypoints.

Quantify in training	add noise	PSNR(Y)	Smoothness
No	-	36.04	**0.85**
Yes	No	<u>36.06</u>	0.81
Yes	Yes	**36.47**	<u>0.83</u>

3.3. Ablation Studies

As mentioned in Section 2.1, Forward Prediction and Forward+Backward Prediction have the disadvantage of generating unsmooth video, so we propose the Pixel-wise Bi-Prediction method. To demonstrate its effectiveness, we compare these three prediction methods, and show results in Table 4, where the Pixel-wise Bi-Prediction method achieves the highest PSNR(Y) score and has the best performance in video smoothness. In Figure 7, we visualize the intermediate products generated in the inference process. It can be found that the predicted mask M_t tends to trust the frame predicted by the key frame that looks more like F_t, which makes sense. For example, in the first row, F_{k1} looks more like F_t than F_{k2}, so the predicted mask gives more weight to F'_{t1} than F'_{t2}.

We also conduct an ablation study in Table 5 to demonstrate the necessity of quantifying keypoints during training and the necessity of adding uniform noise to simulate the quantization loss. In Table 5, quantifying keypoints only in the testing phase results in relatively bad objective performance. Quantifying keypoints in the training phase without adding noise leads to an obvious decline in *smoothness* score. By contrast, quantifying keypoints in the training phase and adding uniform noise to simulate the quantization loss achieves satisfactory performance in both objective and subjective experiments.

4. CONCLUSION

In this paper, we propose a hybrid compression scheme for face video, which combines the pixel-level precise recovery capability of traditional coding with the generation capability of deep learning based on abridged information, achieving the purpose of high quality face video synthesis at ultra-low bitrate. Our proposed Pixel-wise Bi-Prediction method helps generate smooth videos, greatly improving our subjective experience. Without introducing any additional bitrate, a series of completely fair experiments have demonstrated the effectiveness of our proposed scheme. Moreover, this scheme has the characteristic of dynamically-adjustable bitrate and adapts to any existing encoder/configuration to deal with different encoding requirements, resulting in a strong practicability. Our future work includes better keypoint compression method and delay optimization.

Acknowledgements

This work was supported in part by MoE-China Mobile Research Fund Project under Grant MCM20180702, the National Key Research and Development Project of China under Grant 2019YFB1802701, Chinese National Science Funding 62132006, and Shanghai Key Laboratory of Digital Media Processing and Transmissions.

5. REFERENCES

[1] "Versatile video coding," *Rec. ITU-T H.266 and ISO/IEC 23090-3 (VVC)*, August 2020.

[2] "High efficiency video coding," *Rec. ITU-T H.265 and ISO/IEC 23008-2 (HEVC)*, April 2013.

[3] Dahu Feng, Yan Huang, Yiwei Zhang, Jun Ling, Anni Tang, and Li Song, "A generative compression framework for low bandwidth video conference," in *2021 ICMEW*, July 2021, pp. 1–6.

[4] Ting-Chun Wang, Arun Mallya, and Ming-Yu Liu, "One-shot free-view neural talking-head synthesis for video conferencing," in *CVPR*, June 2021, pp. 10039–10049.

[5] Maxime Oquab, Pierre Stock, Daniel Haziza, Tao Xu, Peizhao Zhang, Onur Celebi, Yana Hasson, Patrick Labatut, Bobo Bose-Kolanu, Thibault Peyronel, and Camille Couprie, "Low bandwidth video-chat compression using deep generative models," in *CVPR Workshops*, June 2021, pp. 2388–2397.

[6] Aliaksandr Siarohin, Stéphane Lathuilière, Sergey Tulyakov, Elisa Ricci, and Nicu Sebe, "First order motion model for image animation," in *NeurIPS*, December 2019.

[7] Goluck Konuko, Giuseppe Valenzise, and Stéphane Lathuilière, "Ultra-low bitrate video conferencing using deep image animation," in *ICASSP 2021 - 2021 IEEE International Conference on Acoustics, Speech and Signal Processing (ICASSP)*, 2021, pp. 4210–4214.

[8] Ting-Chun Wang, Ming-Yu Liu, Jun-Yan Zhu, Guilin Liu, Andrew Tao, Jan Kautz, and Bryan Catanzaro, "Video-to-video synthesis," 2018.

[9] Ting-Chun Wang, Ming-Yu Liu, Andrew Tao, Guilin Liu, Jan Kautz, and Bryan Catanzaro, "Few-shot video-to-video synthesis," 2019.

[10] Yuval Nirkin, Yosi Keller, and Tal Hassner, "Fsgan: Subject agnostic face swapping and reenactment," in *ICCV*, 2019, pp. 7184–7193.

[11] Egor Zakharov, Aleksei Ivakhnenko, Aliaksandra Shysheya, and Victor Lempitsky, "Fast bi-layer neural synthesis of one-shot realistic head avatars," in *ECCV*, August 2020.

[12] Adam Wieckowski, Jens Brandenburg, Tobias Hinz, Christian Bartnik, Valeri George, Gabriel Hege, Christian Helmrich, Anastasia Henkel, Christian Lehmann, Christian Stoffers, Ivan Zupancic, Benjamin Bross, and Detlev Marpe, "Vvenc: An open and optimized vvc encoder implementation," in *2021 ICMEW*, 2021, pp. 1–2.

[13] Justin Johnson, Alexandre Alahi, and Li Fei-Fei, "Perceptual losses for real-time style transfer and super-resolution," in *Computer Vision – ECCV 2016*, Cham, 2016, pp. 694–711, Springer International Publishing.

[14] G. G. Langdon, "An introduction to arithmetic coding," *IBM Journal of Research and Development*, vol. 28, no. 2, pp. 135–149, 1984.

[15] Brian Dolhansky, Joanna Bitton, Ben Pflaum, Jikuo Lu, Russ Howes, Menglin Wang, and Cristian Canton Ferrer, "The deepfake detection challenge (dfdc) dataset," 2020.

[16] Joon Son Chung, Arsha Nagrani, and Andrew Zisserman, "Voxceleb2: Deep speaker recognition," *Interspeech 2018*, Sep 2018.

[17] Koki Nagano, Jaewoo Seo, Jun Xing, Lingyu Wei, Zimo Li, Shunsuke Saito, Aviral Agarwal, Jens Fursund, and Hao Li, "Pagan: Real-time avatars using dynamic textures," *ACM Trans. Graph.*, vol. 37, no. 6, dec 2018.

[18] Hyeongwoo Kim, Pablo Garrido, Ayush Tewari, Weipeng Xu, Justus Thies, Matthias Niessner, Patrick Pérez, Christian Richardt, Michael Zollhöfer, and Christian Theobalt, "Deep video portraits," *ACM Transactions on Graphics (TOG)*, vol. 37, no. 4, pp. 1–14, 2018.

[19] Diederik P. Kingma and Jimmy Ba, "Adam: A method for stochastic optimization," *CoRR*, vol. abs/1412.6980, 2015.

In this supplementary, we provide more details and results to make our paper more comprehensive.

A. RELATED WORK

A.1. Traditional Video Compression

In the past few years, many traditional video compression methods have been proposed, such as HEVC [2] and VVC [1]. Based on hybrid video compression framework, traditional methods utilize intra and inter prediction to remove spatial and temporal redundancy by some manually designed schemes. VVC [1] represents the most advanced traditional method. Compared with HEVC [2], VVC can save about 50% of the bitrate while maintaining the similar visual quality. Fraunhofer HHI further released an efficient VVC realization VVenC [12] which has compression performance similar to VVC but with much less encoding complexity.

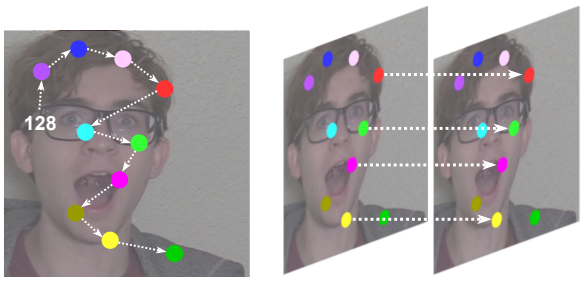
A.2. Deep Talking Head Approaches

Wang et al. proposed the vid2vid [8,9] methods to implement talking head synthesis, but these methods need the transmission of edge maps, which have a relatively high bandwidth cost. The face-reenactment methods [10, 11] also can be applied to implement talking head synthesis. However, the bandwidth cost of the required representations is really high. There are also some 3D-based methods [17, 18] to implement portrait synthesis like DVP [18]. However, this method is subject-specific and needs a thousand images per subject for training. First order model(FOM) [6] uses a representation of a set of learned keypoints along with their local affine transformations to implement the face animation and achieves satisfactory performance especially when the source actor and the target actor share the same identity. Also, the bandwidth cost of FOM [6] is relatively low compared to other methods [8–11]. Based on this, in our method, we designed a low bitrate version of FOM [6]: LowBitrate-FOM (LB-FOM).

B. LOSSLESS CODING SCHEME

In this paper, we let LB-FOM to predict 10 keypoints for each frame. Each keypoint consists of one x coordinate and one y coordinate which is of type Uint8, which means each non-key frame is represented by 20 Bytes if uncompressed. To further compress these values, we design a novel method which reduces the bitrate to 4.98 Bytes per non-key frame. The compression ratio of each step is shown in Table 6.

Intra and Inter Prediction For video sequence, the adjacent frames have high similarity, which may cause information redundancy. We utilize inter prediction to remove the temporal redundancy. As shown in Figure 8(b), we use keypoints in the $(K-1)$th frame to predict the corresponding keypoints in the Kth frame. That means we do not straightly encode the keypoint value of the Kth frame, but encode the residual keypoint value of the $(K-1)$th frame and the Kth frame. For the first non-key frame, we apply intra prediction to remove spatial redundancy. As shown in Figure 8(a), we use the $(N-1)$th keypoint to predict the Nth keypoint. And for the first keypoint in the first non-key frame, we use 128 which is the middle value of coordinate to estimate it. Combined with inter and intra prediction, the bitrate is reduced to 11.7 Bytes per non-key frame.



(a) Intra Prediction. (b) Inter Prediction.

Fig. 8: Intra & Inter Prediction in our lossless coding scheme. Intra Prediction: use $(N-1)$th point to predict Nth point. Inter Prediction: use $(K-1)$th frame to predict Kth frame.

Variable-Length Coding As a Variable-Length Coding algorithm, exponential Golomb coding benefits more when small numbers appear frequently. Duo to keypoints change slightly between adjacent frames, the residual value is small which fits perfectly with the characteristic of exponential Golomb coding. Thus we use zero-order exponential Golomb coding to encode the residual value.

What's more, we use adaptive binary arithmetic coding (an entropy coding) [14] to further reduce the bitrate. At last, the bitrate is reduced to 4.98 Bytes per non-key frame.

C. DELAY ANALYSIS

In this part, we will discuss the delay problem. Suppose the sampling interval is N. When adopting *LDP* (LowDelay-P) mode of VVenC, the delay is (N - 1) frames at the receiver compared to the sender. When adopting *RA* (RandomAccess) mode of VVenC and GOP-size is set to k, the delay is (k*N - 1) frames at the receiver compared to the sender. Consequently, for video conferencing and other scenes with lowdelay requirements, we encode key frames in *LDP* mode. For scenarios that do not have lowdelay requirements such as offline video storage, *RA* mode is also an option.

D. EXPERIMENTAL SETUPS

During training, we apply Adam optimizer [19] with the multi-step learning rate, $\beta_1 = 0.5$ and $\beta_2 = 0.999$. The

Table 6: The compression ratio of each step in our scheme. 1st: remove Jacobian. 2nd: convert data type from Float32 to Uint8. 3rd: Intra & Inter Prediction. 4th: Variable-Length Coding & Arithmetic Coding. Bpf: Bytes-per-frame.

	Origin	1st	2nd	3rd	4th
CompressRatio	-	0.333	0.250	0.585	0.425
non-key-frame / Bpf	240	80	20	11.70	4.98

project is implemented by PyTorch and our training is carried out on 3 NVIDIA TITAN Xp GPUs with batch size 12.

VVenC setups. In *LDP* mode, GOPSize = 8 and IntraPeriod = -1. In *RA* mode, GOPSize = IntraPeriod = 32.

E. COMPLETE EXPERIMENTAL DATA

In RA mode, the complete experimental data of VVenC [12] and our method is shown in Table 7 and Table 8. And in LDP mode, the complete experimental data of VVenC and our method is shown in Table 9 and Table 10. In Table 7 and Table 9, we show the bitrate in three units: bpf (bits-per-frame), bpp (bits-per-pixel) and KBps (1024-Bytes-per-second).

In Table 8 and Table 10, we show the experimental results of our method under different QP values and sampling intervals. For a certain sampling interval, we can divide all frames into two categories: key frames and non-key frames, and the total bitrate is composed of key-frame bitrate and non-key-frame bitrate. From Section B, the bitrate of non-key frames is 20 Bpf (Bytes-per-frame) without compression. With our lossless coding scheme described in Section B, we can compress the non-key-frame bitrate from 20 Bpf to 4.98 Bpf on average. Note that the specific bitrate of non-key frames after compression is slightly different under different sampling intervals. The key frames are seen as a video and are encoded by VVenC with a predefined QP value, so the bitrate of key frames is different when adopting different QP values to compress the key frames. Under a certain sampling interval and QP value, we can calculate the average bitrate according to the corresponding key-frame bitrate and non-key-frame bitrate. In Table 8 and Table 10, we show the bitrate in four units: Bpf (Bytes-per-frame), bpf (bits-per-frame), bpp (bits-per-pixel) and KBps (1024-Bytes-per-second).

From the comparison between Table 7 and Table 8 and the comparison between Table 9 and Table 10, it can be found that compared to VVenC, our method achieves higher PSNR value under the same bitrate and costs lower bitrate when achieving the same PSNR value.

Table 7: Experimental results of VVenC under various QP values. Mode: RA.

QP	32	33	34	35	36	37	38	39	40
bpf	903	817	747	686	631	582	538	502	466
10^{-3}bpp	13.78	12.47	11.40	10.47	9.63	8.88	8.21	7.66	7.11
KBps	3.31	2.99	2.74	2.51	2.31	2.13	1.97	1.84	1.71
PSNR(Y)	39.29	38.81	38.40	37.97	37.51	37.03	36.55	36.05	35.55
QP	42	45	48	50	52	55	58	60	62
bpf	407	341	291	266	246	225	206	200	195
10^{-3}bpp	6.21	5.2	4.44	4.06	3.75	3.43	3.14	3.05	2.98
KBps	1.49	1.25	1.07	0.97	0.9	0.82	0.75	0.73	0.71
PSNR(Y)	34.47	32.83	31.18	30.03	28.93	27.31	25.80	24.91	24.13

Table 8: Experimental results of our method under different QP values and sampling intervals. Mode: RA.

QP	sampling-interval		5	10	20	30	40	50	60	80	100
	non-key-frame / Bpf		5.358	5.079	4.964	4.922	4.907	4.985	4.887	4.876	4.873
27	key-frame / bpf		2949	3648	4822	5859	6448	7173	7984	9149	10315
	average-bitrate	bpf	624.1	401.4	278.8	233.4	199.5	181.8	171.5	152.9	141.7
		10^{-3}bpp	9.52	6.12	4.25	3.56	3.04	2.77	2.62	2.33	2.16
		KBps	2.29	1.47	1.02	0.85	0.73	0.67	0.63	0.56	0.52
	PSNR(Y)		37.98	36.23	34.43	33.33	32.70	32.12	31.49	31.06	30.58
30	key-frame / bpf		2010	2478	3373	4182	4663	5214	5876	6814	7704
	average-bitrate	bpf	436.3	284.4	206.4	177.5	154.8	142.7	136.4	123.7	115.6
		10^{-3}bpp	6.66	4.34	3.15	2.71	2.36	2.18	2.08	1.89	1.76
		KBps	1.6	1.04	0.76	0.65	0.57	0.52	0.5	0.45	0.42
	PSNR(Y)		37.14	35.55	33.92	32.96	32.36	31.87	31.24	30.91	30.45
32	key-frame / bpf		1593	1963	2687	3363	3783	4229	4827	5599	6337
	average-bitrate	bpf	352.9	232.9	172.1	150.2	132.8	123	118.9	108.5	102
		10^{-3}bpp	5.38	3.55	2.63	2.29	2.03	1.88	1.81	1.66	1.56
		KBps	1.29	0.85	0.63	0.55	0.49	0.45	0.44	0.4	0.37
	PSNR(Y)		36.47	35.04	33.58	32.63	32.10	31.60	31.07	30.65	30.30
34	key-frame / bpf		1286	1573	2182	2752	3119	3520	3991	4648	5308
	average-bitrate	bpf	291.5	193.9	146.8	129.8	116.2	108.8	105	96.6	91.7
		10^{-3}bpp	4.45	2.96	2.24	1.98	1.77	1.66	1.6	1.47	1.4
		KBps	1.07	0.71	0.54	0.48	0.43	0.4	0.38	0.35	0.34
	PSNR(Y)		35.75	34.42	33.13	32.24	31.79	31.31	30.85	30.48	30.15
36	key-frame / bpf		1053	1280	1787	2276	2574	2930	3347	3891	4455
	average-bitrate	bpf	244.9	164.6	127.1	113.9	102.6	97	94.2	87.2	83.1
		10^{-3}bpp	3.74	2.51	1.94	1.74	1.57	1.48	1.44	1.33	1.27
		KBps	0.9	0.6	0.47	0.42	0.38	0.36	0.34	0.32	0.3
	PSNR(Y)		34.99	33.81	32.65	31.87	31.41	30.98	30.51	30.21	29.89
38	key-frame / bpf		868	1048	1476	1864	2135	2420	2779	3264	3740
	average-bitrate	bpf	207.9	141.4	111.5	100.2	91.6	86.8	84.3	79.3	76
		10^{-3}bpp	3.17	2.16	1.7	1.53	1.4	1.32	1.29	1.21	1.16
		KBps	0.76	0.52	0.41	0.37	0.34	0.32	0.31	0.29	0.28
	PSNR(Y)		34.14	33.05	32.01	31.26	30.85	30.54	30.10	29.79	29.53

Table 9: Experimental results of VVenC under various QP values. Mode: LDP.

QP	32	33	34	35	36	37	38	39	40
bpf	679	605	542	488	439	398	361	330	301
10^{-3}bpp	10.36	9.23	8.27	7.45	6.7	6.07	5.51	5.04	4.59
KBps	2.49	2.22	1.98	1.79	1.61	1.46	1.32	1.21	1.1
PSNR(Y)	38.00	37.51	37.01	36.50	35.97	35.45	34.92	34.36	33.81
QP	42	45	48	50	52	55	58	60	62
bpf	255	203	169	153	141	130	123	121	112
10^{-3}bpp	3.89	3.1	2.58	2.33	2.15	1.98	1.88	1.85	1.71
KBps	0.93	0.74	0.62	0.56	0.52	0.48	0.45	0.44	0.41
PSNR(Y)	32.71	31.01	29.26	28.12	27.00	25.47	24.11	23.32	22.55

Table 10: Experimental results of our method under different QP values and sampling intervals. Mode: LDP.

QP	sampling-interval		5	10	20	30	40	50	60	80	100
	non-key-frame / Bpf		5.358	5.079	4.964	4.922	4.907	4.895	4.887	4.876	4.873
27	key-frame / bpf		2848	3798	4941	5842	6225	6822	7568	8579	9497
	average-bitrate	bpf	603.9	416.4	284.8	232.8	193.9	174.8	164.6	145.8	133.6
		10^{-3}bpp	9.21	6.35	4.35	3.55	2.96	2.67	2.51	2.22	2.04
		KBps	2.21	1.52	1.04	0.85	0.71	0.64	0.6	0.53	0.49
	PSNR(Y)		37.85	36.23	34.51	33.40	32.71	32.13	31.54	31.11	30.62
30	key-frame / bpf		1910	2575	3387	4062	4364	4822	5377	6190	6889
	average-bitrate	bpf	416.3	294.1	207.1	173.5	147.4	134.8	128.1	115.9	107.5
		10^{-3}bpp	6.35	4.49	3.16	2.65	2.25	2.06	1.95	1.77	1.64
		KBps	1.52	1.08	0.76	0.64	0.54	0.49	0.47	0.42	0.39
	PSNR(Y)		36.85	35.52	33.97	33.02	32.32	31.83	31.30	30.92	30.44
32	key-frame / bpf		1452	1969	2626	3171	3430	3800	4272	4941	5516
	average-bitrate	bpf	324.7	233.5	169	143.8	124	114.4	109.6	100.3	93.8
		10^{-3}bpp	4.95	3.56	2.58	2.19	1.89	1.75	1.67	1.53	1.43
		KBps	1.19	0.86	0.62	0.53	0.45	0.42	0.4	0.37	0.34
	PSNR(Y)		36.10	34.89	33.53	32.58	32.09	31.60	31.05	30.62	30.30
34	key-frame / bpf		1155	1575	2114	2563	2784	3100	3526	4057	4559
	average-bitrate	bpf	265.3	194.1	143.4	123.5	107.9	100.4	97.2	89.2	84.2
		10^{-3}bpp	4.05	2.96	2.19	1.88	1.65	1.53	1.48	1.36	1.28
		KBps	0.97	0.71	0.53	0.45	0.4	0.37	0.36	0.33	0.31
	PSNR(Y)		35.30	34.31	33.04	32.19	31.70	31.28	30.80	30.53	30.10
36	key-frame / bpf		925	1261	1700	2088	2264	2524	2881	3325	3760
	average-bitrate	bpf	219.3	162.7	122.7	107.7	94.9	88.9	86.5	80.1	76.2
		10^{-3}bpp	3.35	2.48	1.87	1.64	1.45	1.36	1.32	1.22	1.16
		KBps	0.8	0.6	0.45	0.39	0.35	0.33	0.32	0.29	0.28
	PSNR(Y)		34.45	33.60	32.46	31.72	31.28	30.92	30.48	30.14	29.88
38	key-frame / bpf		744	1016	1379	1706	1862	2072	2377	2756	3117
	average-bitrate	bpf	183.1	138.2	106.7	94.9	84.8	79.8	78.1	73	69.8
		10^{-3}bpp	2.79	2.11	1.63	1.45	1.29	1.22	1.19	1.11	1.07
		KBps	0.67	0.51	0.39	0.35	0.31	0.29	0.29	0.27	0.26
	PSNR(Y)		33.57	32.82	31.83	31.09	30.79	30.40	30.06	29.85	29.54